

Article

Experimental Analysis of Wireless Power Transmission with Spiral Resonators

Giovanni Puccetti *, Ugo Reggiani and Leonardo Sandrolini

Department of Electrical, Electronic, and Information Engineering “Guglielmo Marconi”,
University of Bologna, Viale del Risorgimento 2, Bologna I-40136, Italy;
E-Mails: ugo.reggiani@unibo.it (U.R.); leonardo.sandrolini@unibo.it (L.S.)

* Author to whom correspondence should be addressed; E-Mail: giovanni.puccetti2@unibo.it;
Tel.: +39-051-20-93578; Fax: +39-051-20-93588.

Received: 29 August 2013; in revised form: 22 October 2013 / Accepted: 4 November 2013 /
Published: 11 November 2013

Abstract: In this paper, a theoretical and experimental analysis of wireless power transfer through a coplanar resonator array is presented. In particular, six identical spiral resonators are used to form an array and transfer power between an emitter and a receiver. All the spiral resonators resonate at about 20 MHz and the emitter and receiver coils are designed with formulas taken from literature. The resonator system is modeled using mutual inductances, being retardation not significant. The transmission coefficient is measured for four different arrangements of the six resonators and the experimental measurements are compared with the theoretical predictions, showing similar trends. The paper shows that the peaks of the transmission coefficient vary slightly for the resonator arrangements considered.

Keywords: spiral resonators; wireless power transfer; transmission coefficient; experimental analysis

1. Introduction

Wireless power transmission has gained a significant interest among researchers and tech industries in recent years [1,2]. To date, however, although this power transfer methodology has been extensively developed for the power supply of electronic devices, a lot of important problems have to be solved from a practical point of view as, for example, the low transmission efficiency when the distance between the emitter and receiver coils is larger than a few tens of centimeters or the two coils are misaligned.

Recent studies have shown that the presence of interposed metamaterials or resonators can improve the efficiency of the wireless power transfer, channeling the magnetic field in resonance condition [3–5]. Arrays of resonators are used for this purpose and lately they have been studied by many researchers through the theory of magnetoinductive waves [6–8]. Generally, the resonators are disposed with parallel axes to form an axial or planar structure and with the emitter and receiver coils facing the structure, but it is still a very important and current issue to analyse their spatial arrangement [9,10]. An experimental study concerning the effects of the insertion of spiral resonators (SRs) between the emitter and receiver coils is presented in this paper and measurement of the transmission coefficient S_{21} for different SR arrangements and distances between the emitter and receiver coils is performed. More precisely, in Section 2, theoretical aspects concerning the design of spiral resonators and the equivalent electric circuit of a wireless power transmission system with interposed SRs are given. In Sections 3 and 4, the experimental apparatus and the results of the transmission coefficient are presented, and some comparisons between measures and theoretical predictions are performed.

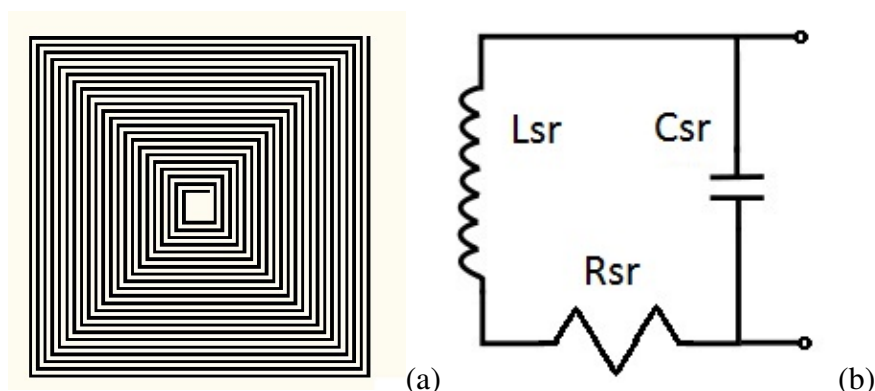
2. Design of SR and Equivalent Circuit

A spiral resonator is a loop etched or milled on a printed circuit board (PCB) that some authors point out as a resonator or metamaterial having one of the lowest resonant frequency achievable [11,12]. In Figure 1a the typical geometry of a SR of square shape and straight side and in Figure 1b its quasi-static equivalent electric circuit are shown. SRs of more complex geometry, such as planar zig-zag spiral resonators [13], could be considered. In Figure 1b L_{SR} is the self-inductance of the loop, consisting of N turns formed with lands on a PCB, C_{SR} represents the equivalent stray capacitance distributed between adjacent turns and R_{SR} is the loop resistance considered as a function of frequency. In this equivalent electric circuit, the high-order effects (for example, the stray capacitance between nonadjacent turns) are neglected. The nominal self-resonant frequency of a resonator is calculated from [14]:

$$f_{0th} = \frac{1}{2\pi\sqrt{L_{SR}C_{SR}}} \quad (1)$$

where L_{SR} and C_{SR} can be calculated with good agreement through the method of “partial” inductance [15] and the formula proposed in [16], respectively.

Figure 1. (a) An example of SR with $N = 22$ turns; (b) Quasi-static equivalent electric circuit of the SR structure.



For a multiple resonator system, the equivalent circuit becomes more complex and the mutual impedances between each couple of resonators are essential parameters. Consider a system in which n identical magnetic coupled resonators are interposed between the emitter and receiver coils. If both the period and the total length of the structure are much smaller than the free-space wavelength at the operating frequency (see Section 3), the retarding effects can be neglected and consequently the mutual impedances between two resonators and each resonator and a coil are purely imaginary, *i.e.*, only the mutual inductances, due to magnetic coupling, are effective [9]. Then, if only the emitter coil is supplied, the multiple resonator system is shown in Figure 2 and its equivalent electrical circuit can be represented in matrix form through the following equation:

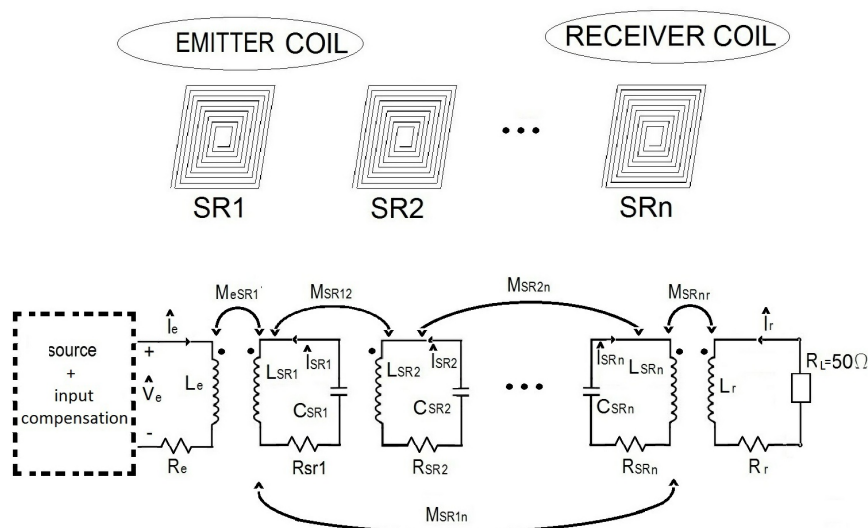
$$\hat{\mathbf{V}} = \hat{\mathbf{Z}}\hat{\mathbf{I}} \tag{2}$$

where $\hat{\mathbf{V}} = [\hat{V}_e \ 0 \ \dots \ 0]^T$ with \hat{V}_e phasor supply voltage of the emitter coil, $\hat{\mathbf{I}}$ is the inductor current complex vector, and $\hat{\mathbf{Z}}$ is the symmetric matrix of the impedances defined as follows:

$$\begin{bmatrix} \hat{Z}_e & j\omega M_{eSR1} & \dots & j\omega M_{eSRn} & j\omega M_{er} \\ j\omega M_{SR1e} & \hat{Z}_{SR1} & \dots & j\omega M_{SR1n} & j\omega M_{SR1r} \\ \vdots & \vdots & \ddots & \vdots & \vdots \\ j\omega M_{SRne} & j\omega M_{SRn1} & \dots & \hat{Z}_{SRn} & j\omega M_{SRnr} \\ j\omega M_{re} & j\omega M_{rSR1} & \dots & j\omega M_{rSRn} & \hat{Z}_r \end{bmatrix} \tag{3}$$

where $\hat{Z}_{e(r)} = R_{e(r)} + j\omega L_{e(r)}$ and $\hat{Z}_{SRn} = R_{SRn} + j\omega L_{SRn} + 1/j\omega C_{SRn}$ represent the impedance of each inductor. In particular, the subscript e (r) identifies the electrical parameter of the emitter (receiver) coil. The emitter and receiver coils are designed with the procedure presented in [17] which allows their electrical parameters to be calculated analytically. The mutual inductances between each couple of inductors in the system are calculated with good approximation following the method proposed in [18]. The frequency-dependent resistance R_{SR} of the identical resonators is calculated by the formula proposed in [16].

Figure 2. Schematic of a wireless power transmission system with n coupled resonators and its equivalent electric circuit.



3. Experimental Setup

For the analysis of the transmitted power, six identical samples of SR designed to resonate at about 20 MHz were used. Furthermore, two equal solenoid coils were made as emitter and receiver coils. The experimental setup and the coils used as emitter and receiver are shown in Figure 3a,b, respectively. The two coils are made of 2 turns of a circular cross-section wire of 1 mm diameter; the coil diameter is 70 mm and the turn-to-turn distance is 0.3 mm. The SRs have a length of the outer side of 80 mm, a land width of 0.4 mm, 28 turns and a distance between two adjacent turns of 0.9 mm. The period and the total length of the resonator system are 85 mm and 505 mm, respectively. The emitter and receiver coils were connected to the output and input ports of a R&S ESRP test receiver (Rohde & Schwarz, Munich, Germany) 10 Hz–7 GHz with tracking generator, respectively.

Figure 3. (a) Experimental setup; (b) Solenoid coils used as emitter (left) and receiver (right) in transmitted power tests.



The calculated self-inductance of the emitter (receiver) coil is $L_{e(r),cal} = 0.74 \mu\text{H}$ while the measured value is $L_{e(r),m} = 0.76 \mu\text{H}$. The calculated electrical parameters of the SRs are $L_{SR,cal} = 30.0 \mu\text{H}$ and $C_{SR,cal} = 2.24 \text{ pF}$. The measured self-inductance of the resonators is $L_{SR,m} = 28.9 \mu\text{H}$. Table 1 shows the measured self-resonant frequency f_{0m} and the experimental capacitance $C_{SR,m}$ for each SR sample. The measures of the self-resonant frequencies were performed with the R&S ESRP test receiver (Rohde & Schwarz, Munich, Germany). The self-inductances of the coils and SRs were measured with a HP 4192 A impedance analyzer (Agilent Technologies, Inc., Santa Clara, CA, USA). The values of $C_{SR,m}$ are obtained introducing the values of $L_{SR,m}$ and f_{0m} into Equation (1).

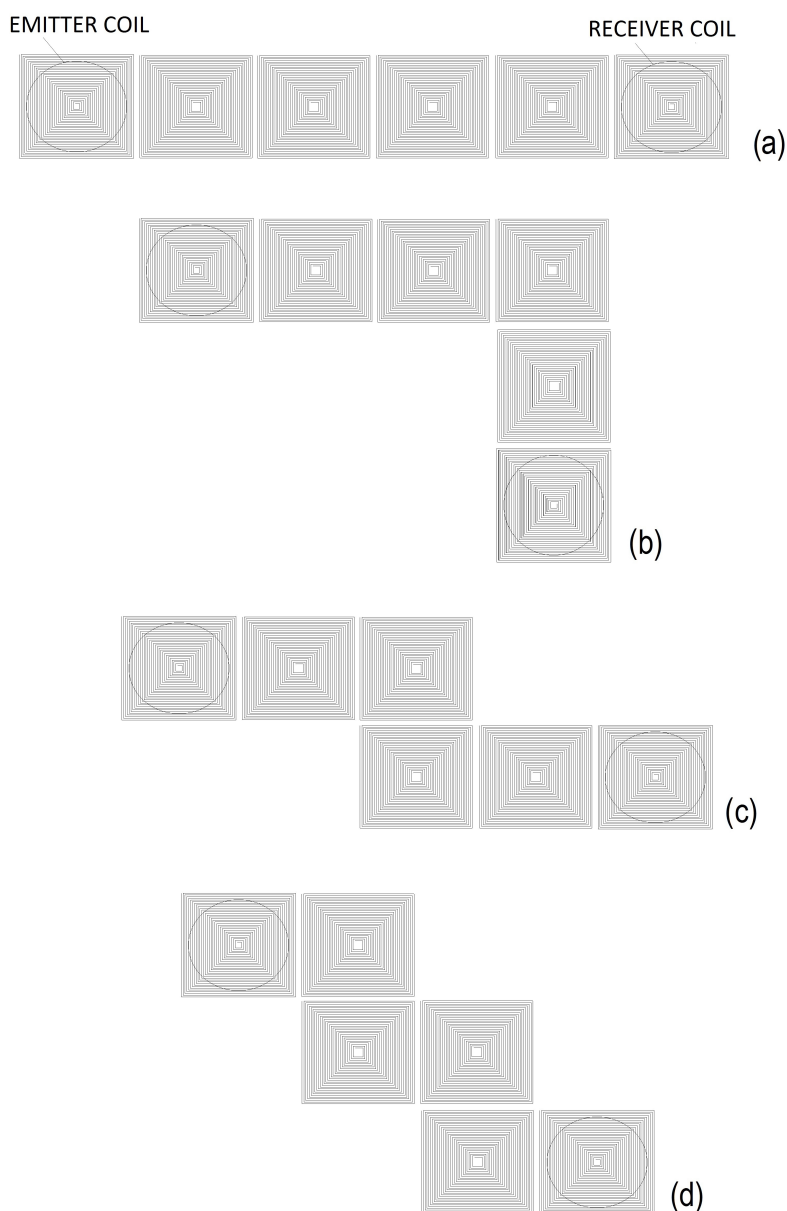
Table 1. Measured self-resonant frequency f_{0m} and experimental capacitance $C_{SR,m}$ for each SR sample.

Sample	f_{0m} [MHz]	$C_{SR,m}$ [pF]
SR1	19.55	2.28
SR2	19.56	2.28
SR3	19.52	2.29
SR4	19.52	2.29
SR5	19.52	2.29
SR6	19.3	2.34

The theoretical self-resonant frequency of the resonators f_{0th} , calculated introducing $L_{SR,cal}$ and $C_{SR,cal}$ into Equation (1), is 19.4 MHz; the error between the values of the self-resonant frequency calculated and measured is less than 5%. The Q factor of each resonator was estimated about 230 at the resonant frequency.

The experiments were performed in order to analyse the transmission coefficient in an array of resonators and its variation for different arrangements of the array. Hence, four different coplanar combinations were tested maintaining the same number of SRs. The different arrangements considered are shown in Figure 4.

Figure 4. Representation of the four arrangements tested: (a) I-arrangement; (b) II-arrangement; (c) III-arrangement and (d) IV-arrangement. The receiver coil is moved along the SR array.



In each test, the distance between two adjacent SRs was 5 mm so the coupling coefficient is calculated as $k_{SR} = 2M_{SR}/L_{SR} \approx 0.11$. Furthermore, as the receiver coil is connected to a spectrum analyzer having an input impedance $R_L = 50 \Omega$, the receiver coil was matched to the structure at its end when it was positioned above the last resonator. This situation was achieved by choosing the distance between the receiver coil and the SR equal to 23 mm so as to satisfy the condition [19]:

$$M_{SRnr} = \sqrt{\frac{M_{SR}}{2\pi f_{0th}} R_L} \tag{4}$$

The emitter coil was placed at the same distance from the array of resonators. The relevant coupling coefficient is almost $k_{e(r)SR} = M_{rSR}/\sqrt{L_r L_{SR}} \approx 0.17$.

4. Results

The analysis of the transmission coefficient S_{21} was developed comparing experimental measurements with analytically predicted results obtained with a Scilab computer code [20]. The matrix of impedances Equation (3) becomes as follows:

$$\begin{bmatrix} \hat{Z}_e & j\omega M_{eSR1} & \dots & j\omega M_{eSR3} & \dots & j\omega M_{eSR5} & \dots & j\omega M_{er} \\ j\omega M_{SR1e} & \hat{Z}_{SR1} & \dots & j\omega M_{SR13} & \dots & j\omega M_{SR15} & \dots & j\omega M_{SR1r} \\ \vdots & \vdots & \ddots & \vdots & \ddots & \vdots & \ddots & \vdots \\ j\omega M_{SR3e} & j\omega M_{SR31} & \dots & \hat{Z}_{SR3} & \dots & j\omega M_{SR35} & \dots & j\omega M_{SR3r} \\ \vdots & \vdots & \ddots & \vdots & \ddots & \vdots & \ddots & \vdots \\ j\omega M_{SR5e} & j\omega M_{SR51} & \dots & j\omega M_{SR53} & \dots & \hat{Z}_{SR5} & \dots & j\omega M_{SR5r} \\ \vdots & \vdots & \ddots & \vdots & \ddots & \vdots & \ddots & \vdots \\ j\omega M_{re} & j\omega M_{rSR1} & \dots & j\omega M_{rSR3} & \dots & j\omega M_{rSR5} & \dots & \hat{Z}_r \end{bmatrix} \tag{5}$$

Clearly, the values of the mutual inductances depend on the type of the system under test. Solving Equation (2) with the impedance matrix given by Equation (5), it is possible to obtain the current I_r in the receiver coil and so the transmitted power $50I_r^2$, being 50Ω the input impedance of the spectrum analyzer to which the receiver coil was connected.

In Figure 5, the transmission coefficient S_{21} as a function of frequency for the arrangements I and II is shown. As in each test the emitter coil is fixed in front of SR1, the results depend on the position of the receiver coil and the arrangement of the resonators under consideration. If the measured patterns are compared with the analytically predicted ones, the trends are in agreement in particular under resonance condition. These results are performed for the distance of 23 mm between the receiver coil and the array that realizes the matching condition.

Figure 6 shows the peaks of the transmission coefficient S_{21} for each arrangement of the resonators and position of the receiver coil for the distance of 23 mm. In particular, with reference to the calculated values, the S_{21} peak is higher when there is a direct coupling between the emitter and the receiver coil located above SR2. A general decay of the S_{21} peaks occurs moving the receiver coil along the SR array as the mismatching of the system generates standing waves. After a minimum value is reached, the S_{21}

peak increases and a new maximum value is obtained on top of SR6. Moreover, the system has a low efficiency (between about 20% and 35%) due to the weak magnetic coupling between the resonators. However, considering each arrangement of the array, it can be noticed that the calculated values of the peaks vary in a narrow range. The results obtained are corroborated by the results of the simulations presented in [6]. The measurements of the S_{21} peaks show a trend similar to the calculations with a minimum along the array although the difference between measured and calculated values increases approaching the end of the array. This difference in the trends may be related to the different resistance values of the SRs due to imperfections determined by the fabrication process. Further investigations are needed on this point.

In Table 2, all the values of the measured f_m and calculated f_{th} frequencies of the S_{21} peaks are reported. It is important to observe that both the measured and calculated values of the frequencies at which the peaks occur are slightly different due to standing waves which arise when the receiver coil is not above SR6 in matching condition. Anyway, the values of the peak frequencies are similar for each receiver position, regardless of the type of arrangement. It can be noted that the theoretical frequencies when the receiver coil is on the top of the SR6 are nearly coincident regardless of the arrangement; the same result is obtained in the experiments, thus showing that an adequate matching condition was achieved.

Figure 5. Measured and calculated transmission coefficient S_{21} as a function of frequency. These trends are for I-arrangement (a) and II-arrangement (b) when the receiver coil is facing the SR6.

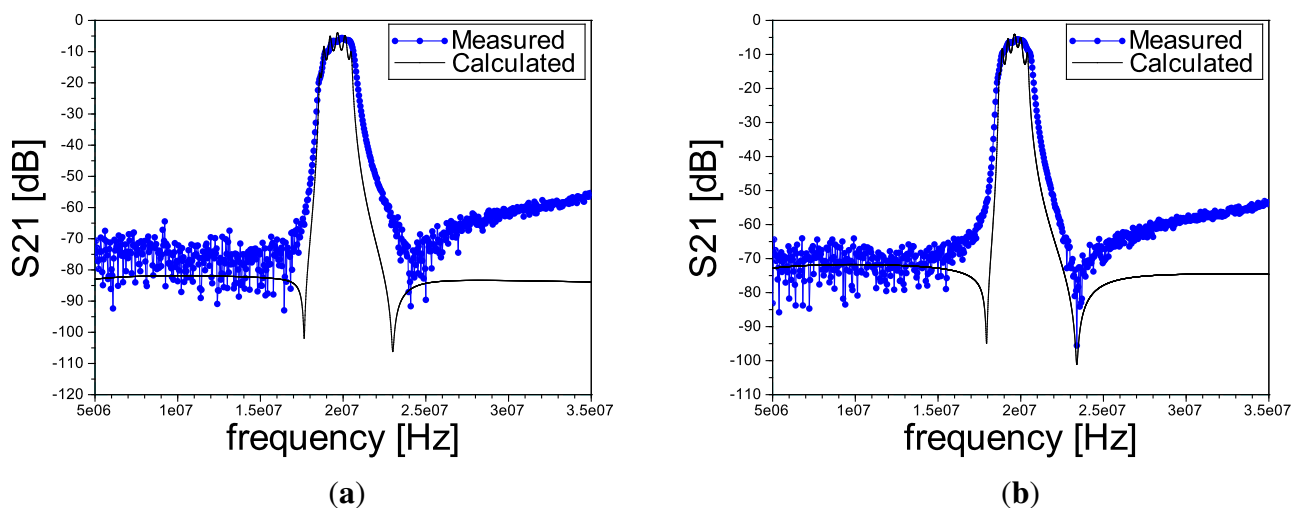


Figure 6. Measured and calculated peaks of the transmission coefficient S_{21} as a function of the position of the receiver coil for each arrangement of the array of SRs. (a) I-arrangement; (b) II-arrangement; (c) III-arrangement and (d) IV-arrangement.

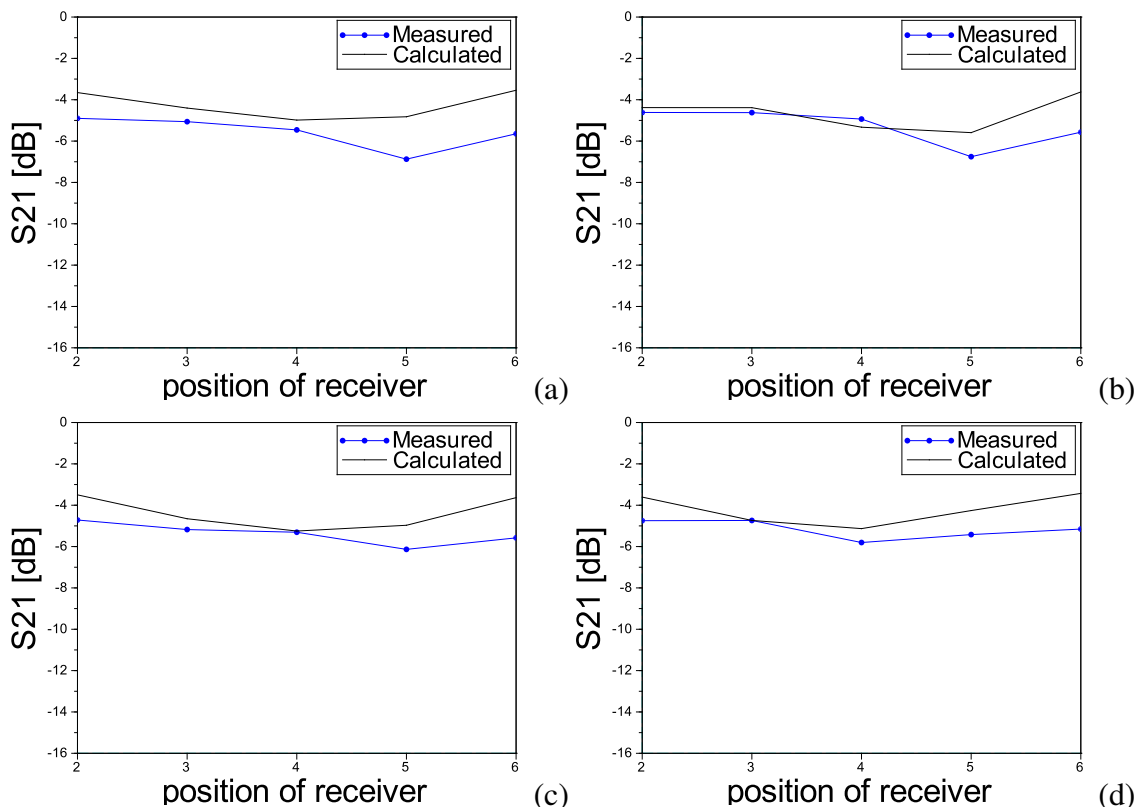


Table 2. Values of the measured f_m and calculated f_{th} frequencies [MHz] of the S_{21} peaks as a function of the arrangement of the SR array and position of the receiver.

Receiver	I		II		III		IV	
	f_m	f_{th}	f_m	f_{th}	f_m	f_{th}	f_m	f_{th}
SR2	19.4	20.7	19.3	20	19.3	20	19.3	20
SR3	19.9	19.7	19.8	19.7	19.8	19.7	19.7	19.6
SR4	19.7	20.5	19.4	20.6	19.6	19.2	19.3	19
SR5	19.3	20.2	19.3	20.2	20.2	20.1	20.2	19
SR6	20	19.6	19.8	19.6	19.9	19.6	19.8	19.5

5. Conclusions

In this paper, a theoretical and experimental analysis of wireless power transfer through an array of coplanar resonators is presented. In particular, six identical SRs were used to form an array and transfer power between an emitter and a receiver. The spiral resonators are designed to resonate at about 20 MHz. Hence, the transmission coefficient is measured for four different arrangements having the same number of resonators and the experimental results are compared with the theoretical predictions, obtaining an

analogous behaviour with differences that may be related to the resistance values of the SRs, which depend on the fabrication process. The values of the transmission coefficient peaks vary slightly for the considered SR arrangements. About the system efficiency, some considerations are made. First of all, the transmitted power of the system is affected by the weak coupling strength between SRs and between SR and coils. This lack can be reduced by using other configurations (for example axial) or other type of resonators, as shown in [21]. On the other hand, the efficiency along the SR structure is also reduced by the matching condition which is obtained in the last position of the array only. It is possible to improve the efficiency mainly increasing the coupling strength between the receiver coil and SR array so that most power is transmitted. Optimizing the system presented can allow the wireless charging of consumer electronic devices regardless of the receiver position and the arrangement of the SR array.

Conflicts of Interest

The authors declare no conflict of interest.

References

1. Villa, J.L.; Sallan, J.; Llombart, A.; Sanz, J.F. Design of a high frequency inductively coupled power transfer system for electric vehicle battery charge. *Appl. Energy* **2009**, *86*, 355–363.
2. Jang, Y.; Jovanovic, M. A contactless electrical energy transmission system for portable telephone battery chargers. *IEEE Trans. Ind. Electron.* **2003**, *50*, 520–527.
3. Wang, B.; Ellstein, D.; Teo, K.H. Analysis on Wireless Power Transfer to Moving Devices Based on Array of Resonators. In Proceedings of the European Conference Antennas and Propagation (EUCAP), Prague, Czech Republic, 26–30 March 2012.
4. Choi, J.; Seo, C. High-efficiency wireless energy transmission using magnetic resonance based on metamaterial with relative permeability equal to -1 . *Prog. Electromagn. Res.* **2010**, *106*, 33–46.
5. Wang, B.; Yerazunis, W.; Teo, K.H. Wireless power transfer: Metamaterials and array of coupled resonators. *IEEE Proc.* **2013**, *101*, 1359–1368.
6. Stevens, C.J. Power Transfer via metamaterials. *CMC: Comput. Mater. Cont.* **2013**, *33*, 1–18.
7. Shamonina, E.; Kalinin, V.A.; Ringhofer, K.H.; Solymar, L. Magneto-inductive waveguide. *Electron. Lett.* **2002**, *38*, 371–373.
8. Stevens, C.J.; Chan, C.W.T.; Stamatis, K.; Edwards, D.J. Magnetic metamaterials as 1-D data transfer channels: An application for magneto-inductive waves. *IEEE Trans. Microw. Theory Tech.* **2010**, *58*, 1248–1256.
9. Radkovskaya, A.; Sydoruk, O.; Shamonin, M.; Stevens, C.J.; Faulkner, G.; Edwards, D.J.; Shamonina, E.; Solymar, L. Transmission properties of two shifted magnetoinductive waveguides. *Microw. Opt. Technol. Lett.* **2007**, *49*, 1054–1058.
10. Lee, C.K.; Zhong, W.X.; Hui, S.Y.R. Effects of magnetic coupling of nonadjacent resonators on wireless power domino-resonator systems. *IEEE Trans. Power Electron.* **2012**, *27*, 1905–1912.

11. Ekmekci, E.; Turhan-Sayan, G. Reducing the Electrical Size of Magnetic Metamaterial Resonators by Geometrical Modifications: A Comparative Study for Single-Sided and Double-Sided Multiple SRR, Spiral and U-Spiral Resonators. In Proceedings of the Antennas and Propagation Society International Symposium (AP-S 2008), San Diego, CA, USA, 5–11 July 2008.
12. Alici, K.B.; Bilotti, F.; Vegni, L.; Ozbay, E. Miniaturized negative permeability materials. *Appl. Phys. Lett.* **2007**, *91*, 1–3.
13. Sandrolini, L.; Reggiani, U.; Puccetti, G. Analytical calculation of the inductance of planar zig-zag spiral inductors. *Prog. Electromagn. Res.* **2013**, *142*, 207–220.
14. Zhong, W.; Lee, C.K.; Hui, S.Y. General analysis on the use of Tesla's resonators in domino forms for wireless power transfer. *IEEE Trans. Ind. Electron.* **2013**, *60*, 261–270.
15. Paul, C.R. *Inductance: Loop and Partial*; John Wiley & Sons: Hoboken, NJ, USA, 2010.
16. Jow, U.M.; Ghovanloo, M. Design and optimization of printed spiral coils for efficient transcutaneous inductive power transmission. *IEEE Trans. Biomed. Circuits Syst.* **2007**, *1*, 193–202.
17. Sandrolini, L.; Reggiani, U.; Puccetti, G.; Neau, Y. Equivalent circuit characterization of resonant magnetic coupling for wireless transmission of electrical energy. *Int. J. Circuit Theory Appl.* **2013**, *41*, 753–771.
18. Sonntag, C.; Lomonova, E.A.; Duarte, J.L. Implementation of the Neumann formula for Calculating the Mutual Inductance between Planar PCB Inductors. In Proceedings of the International Conference on Electrical Machines (ICEM), Vilamoura, Portugal, 6–9 September 2008.
19. Syms, R.R.A.; Young, I.R.; Solymar, L. Low-loss magneto-inductive waveguides. *J. Phys. D Appl. Phys.* **2006**, *39*, 3945–3951.
20. Scilab, Computer Software. (Version 5.4.0). The Scilab Consortium, 2010. Available online: <http://www.scilab.org> (accessed on 1 October 2012).
21. Solymar, L.; Shamonina, E. *Waves in Metamaterials*; Oxford University Press Inc.: New York, NY, USA, 2009.